

MOL 28407

Motexafin Gadolinium-Induced Cell Death Correlates with HO1 Expression and Inhibition of P450 Reductase-Dependent Activities

John P. Evans, Fengyun Xu, Mint Sirisawad, Richard Miller, Louie Naumovski and Paul
R. Ortiz de Montellano

Department of Pharmaceutical Chemistry, University of California, 600 16th Street, San
Francisco, CA 94158-2517, U.S.A. (J.P.E., F.X., P.R.O.M.)

Pharmacyclics, Inc., 995 Arques Ave. Sunnyvale, CA 94085, U.S.A. (M.S., R.M., L.N.)

MOL 28407

Running Title: P450 reductase inhibition and anticancer activity

Address editorial correspondence to:

Paul Ortiz de Montellano
University of California, San Francisco
600 16th Street
San Francisco, CA 94143-2280
U.S.A.
TEL: (415) 476-2903
FAX: (415) 502-4728
email: ortiz@cgl.ucsf.edu

Number of

Text pages: 30

Tables: 0

Figures: 9

References: 41

Words in Abstract: 199

Words in Introduction: 516

Words in Discussion: 1,105

Abbreviations: BVR, biliverdin reductase; CPR, NADPH-cytochrome P450 reductase; HO1, heme oxygenase-1; MGd, motexafin gadolinium; NHE, normal hydrogen electrode; ROS, reactive oxygen species; SOD, superoxide dismutase; SnPPIX, tin protoporphyrin IX.

MOL 28407

Abstract

Heme oxygenase-1 (HO1), which oxidizes heme to biliverdin, CO, and free iron, conveys protection against oxidative stress and is antiapoptotic. Under stress conditions, some porphyrin derivatives can inhibit HO1 and trigger cell death. Motexafin gadolinium (MGd) is an expanded porphyrin that selectively targets cancer cells through a process of futile redox cycling that decreases intracellular reducing metabolites and protein thiols. Here, we report that hematopoietic-derived cell lines that constitutively express HO1 are more susceptible to MGd-induced apoptosis than those that do not. MGd used in combination with tin protoporphyrin IX, an inhibitor of HO1, resulted in synergistic cell killing. Consistent with these cell culture observations, we found that MGd is an inhibitor of heme oxygenase-1 activity *in vitro*. We demonstrate that inhibition of HO1 reflects an interaction of MGd with NADPH-cytochrome P450 reductase, the electron donor for HO1, that results in diversion of reducing equivalents from heme oxidation to oxygen reduction. In accord with this mechanism, MGd is also an *in vitro* inhibitor of CYP2C9, CYP3A4, and CYP4A1. Inhibition of HO1 by MGd may contribute to its anticancer activity, while its *in vitro* inhibition of a broad spectrum of P450 enzymes indicates that a potential exists for drug-drug interactions.

MOL 28407

Motexafin gadolinium (MGd, Xcytrin[®]) is a pentaaza-coordinated expanded porphyrin with biological activity as an anti-cancer agent (**Fig. 1A**). It selectively localizes to cancerous cells (Young et al., 1996), a characteristic inherent to many porphyrins, and facilitates their destruction through redox processes that generate reactive oxygen species (ROS) and deplete the cell of reducing factors (Magda et al., 2002; Magda et al., 2001). In the presence of ascorbate, nicotinamide adenine dinucleotide phosphate (NADPH) or glutathione (GSH), MGd is easily reduced ($E_{1/2}(\text{red}) \approx 0.08 \text{ V vs NHE}$) (Ali and van Lier, 1999). Under aerobic conditions, MGd in turn reduces O_2 to superoxide, which can disproportionate to hydrogen peroxide (**Fig. 1B**). This redox cycling is only part of the toxicity of MGd since enzymes with redox-active cysteine residues such as ribonucleotide reductase and thioredoxin reductase are inhibited by MGd with IC_{50} 's in the low μM range (Hashemy et al., 2006).

Heme degradation is catalyzed by the microsomal enzyme HO1 and requires NADPH and O_2 for oxidative cleavage of the porphyrin ring at the α -methylene carbon to produce α -biliverdin, CO and free iron (Ortiz de Montellano, 1998). Cytochrome P450 reductase (CPR) is required to mediate the flow of electrons from NADPH to HO1. The biliverdin product is subsequently reduced by biliverdin reductase (BVR) to bilirubin, a potent antioxidant (Stocker et al., 1987). HO1 is induced by a number of factors typical of cancer cells, including heme, oxidative stress, and hypoxia (Choi and Alam, 1996). The primary determinants of the substrate specificity of HO1 are the two propionate groups at C6 and C7 of the heme (Tomaro et al., 1984), although recently compounds based on azalanstat, a structure dissimilar to heme, have been shown to be effective HO1 inhibitors (Vlahakis et al., 2005).

MOL 28407

Inhibition of HO1 has been shown to result in antitumor activity, presumably through inactivation of the antiapoptotic properties of the products of HO1 (Sahoo et al., 2002; Tanaka et al., 2003; Berberat et al., 2005). Since MGd is an expanded porphyrin with some structural resemblance to heme and it is cytotoxic to some cell lines, we determined whether MGd is capable of inhibiting HO1 (Chen et al., 2005). We have found that MGd is only cytotoxic to hematopoietic cell lines that express HO1 constitutively. We have also determined the inhibitory effects of MGd on HO1 under a variety of *in vitro* conditions. We conclude that the high electron affinity of the molecule rather than its structural similarities to heme lead to inhibition of HO1 activity. This inhibition is starkly greater in the presence of CPR. As CPR is the mandatory electron donor for almost all human cytochrome P450 enzymes, we have also examined the effects of MGd on the catalytic turnover of these enzymes. We have found that MGd is also an active inhibitor of cytochrome P450 enzymes, although with a lower potency than that exhibited for inhibition of HO1. This suggests that MGd may inhibit a broad range of enzymes that depend on O₂ and cellular reducing equivalents for activity. The interplay of HO1 and MGd may therefore be highly relevant to the anticancer action of MGd.

MOL 28407

Materials and Methods

Materials - Sodium ascorbate, deferoxamine, hemin, NADPH, and glucose-6-phosphate were purchased from Sigma (St. Louis, MO). Methanol (HPLC grade) was from Fisher Scientific. MGd was formulated by Pharmacyclics, Inc. (Sunnyvale, CA) as a 2 mM stock solution in 5% aqueous mannitol. SnPPIX dichloride was from Frontier Scientific, Inc. (Logan, UT).

Cell Line and Growth Conditions - HF-1, Ramos, DHL-4, DB and Raji are B-cell derived tumor lines. HL-60 is a myeloid line, while Jurkat and HuT78 are T-cell derived. Wil-2 is a B-lymphoblastoid cell line. All cell lines were grown in RPMI 1640 with 10% fetal bovine serum in a 5% CO₂/air incubator at 37 °C. For assays determining HO1 induction, growth inhibition or apoptosis, cells were treated with 50 μM of MGd for 24 h prior to analysis.

Analysis of MGd Treated Cells - Cell numbers were determined using a Model Z2 counter (Beckman-Coulter, Miami, FL). Annexin V binding and propidium iodide exclusion were assayed with a FACSCalibur instrument (Becton-Dickinson, San Jose, CA) using reagents from BioVision (Mountain View, CA) per manufacturer's protocol.

For drug combination studies, cytotoxicity was evaluated using annexin-V staining. This data was then entered into CalcuSyn software (Biosoft, Ferguson, MO) for analysis by the combination index (CI) method of Chou and Talalay to determine synergism (CI < 1), additivity (CI = 1) or antagonism (CI > 1) (Chou and Talalay, 1983).

MOL 28407

Western Blotting for Heme Oxygenases - Cells were lysed in triple-detergent lysis buffer [50 mM Tris-Cl (pH 8.0), 150 mM NaCl, 0.1% SDS, 0.5% deoxycholic acid, 1.0% NP-40, supplemented with 1 mM phenylmethylsulphonylfluoride (PMSF) and the COMPLETE protease inhibitor cocktail (Roche Molecular Biochemicals, Indianapolis, IN)] on ice for 10 min. After centrifugation at 10,000 \times g for 10 min, the protein concentration was quantitated in the supernatant and equal quantities of protein were resolved on the appropriate percentage SDS-polyacrylamide gels (Bio-Rad, Hercules, CA). Gels were transferred to polyvinylidene difluoride membranes using a Semi-dry Transfer Cell (Bio-Rad, Hercules, CA) and western blotting was performed using primary and anti-mouse and anti-rabbit secondary antibodies conjugated to AlexaFluor680 (Molecular Probes, Eugene, OR) and IRdye800 (Rockland Immunochemicals, Gilbertsville, PA), respectively. All membranes were blotted with an anti-Hsc70 (Santa Cruz Biotechnology, Inc., Santa Cruz, CA) antibody to control for loading and transfer. Bands were imaged and quantified in the linear range and normalized to Hsc70, using an Odyssey Infrared Imaging System (LICOR, Lincoln, NE).

Enzymes - Truncated human HO1 lacking the 23 C-terminal residues was expressed, purified and reconstituted with heme as previously described (Wilks et al., 1995). Human CPR was expressed and purified according to published procedures (Dierks et al., 1998), and CYP4A1 was expressed and purified as previously described (Hoch et al., 2000). Vivid CYP3A4 and CYP2C9 screening kits were purchased from Invitrogen (Carlsbad, CA). Catalase, SOD, glucose-6-phosphate dehydrogenase, cytochrome *c*, and protocatechuate 3,4-dioxygenase were purchased from Sigma.

MOL 28407

Spectroscopic Methods - Spectroscopic assays were performed on an Agilent 8453 diode array spectrophotometer in 0.1 M potassium phosphate buffer, pH 7.4, at room temperature (~22 °C). The final concentrations in the assays were 1 μM human CPR, 200 μM NADPH, and 10 μM MGd. The NADPH regenerating system consisted of 5 mM glucose-6-phosphate, and 1 unit/mL of glucose-6-phosphate dehydrogenase. The rates of NADPH and MGd consumption were measured by monitoring the absorption decrease at 340 nm ($\epsilon = 6.22 \text{ mM}^{-1}\text{cm}^{-1}$) and 470 nm ($\epsilon = 85 \text{ mM}^{-1}\text{cm}^{-1}$) for NADPH and MGd, respectively. To measure the stoichiometry of NADPH consumption by MGd, assays containing 400 μM NADPH and 1 μM CPR were mixed with repeated additions of 2 μM MGd. The amounts of NADPH and MGd consumed for each addition were compared.

Measurement of HO1 Activity by HPLC - Assays were carried out in 300 μL of a solution containing 0.1 M potassium phosphate buffer, pH 7.4, 1 μM HO1, 10 μM heme, and either 1 μM CPR, 1 mM NADPH, 5 mM glucose-6-phosphate, and 1 unit/mL glucose-6-phosphate dehydrogenase, or 10 mM sodium ascorbate plus 2 mM deferoxamine. The inhibitor (MGd or SnPPIX) concentrations ranged from 0.1 – 100 μM . In one set of experiments catalase (10 $\mu\text{g}/\text{ml}$) and SOD (17 units/mL) were included. Each reaction was preincubated in the dark for 10 min at room temperature followed by 15 min incubation after addition of the reductant. The reaction was quenched with two drops of hydrochloric acid (37%) and three drops of acetic acid and was extracted with 700 μL of CH_2Cl_2 . The organic phase was washed with 700 μL of water and evaporated under a stream of air. The resulting residue was dissolved in 500 μL of methanol (5% H_2SO_4 v/v) and was maintained at 4 °C for at least 8 h in the dark. The dimethyl-

MOL 28407

esterified biliverdin was extracted with 700 μL of CHCl_3 . The organic phase was washed with water (2 x 700 μL) and was then evaporated to dryness under a stream of air. The residue was dissolved in 70% methanol and was loaded onto a YMC ODS-AQ column (S-5, 120 \AA , 4.5 x 250 mm). Solvents A and B were water and methanol, respectively. The HPLC running conditions were as follows: flow rate, 1.0 mL/min; 30% B for 5 min, 30-70% B in 0.1 min, 70-95% B in 25 min, 95% B for 7 min, 95-30% B in 1 min, and finally 30% B for 20 min. The eluent was monitored at 375 nm and was referenced against the absorption at 598 nm.

Cytochrome c Reduction Assay - Reactions contained 0.1 M potassium phosphate buffer, pH 7.4, 1 μM HO1, 10 μM heme, 1 mM NADPH, and 10 μM MGd in the presence and absence of 1 μM CPR. After 15 min an aliquot of the reaction was diluted 100-fold into a 100 μL assay mixture within a cuvette containing 40 μM cytochrome *c* and 200 μM NADPH, so that the final concentration of CPR was 10 nM and of MGd 100 nM. The increase in absorbance at 550 nm was monitored over 2 min and the rate of cytochrome *c* reduction was calculated using an extinction coefficient for reduced cytochrome *c* of 21 $\text{mM}^{-1} \text{cm}^{-1}$ (Margoliash and Walasek, 1967).

O₂ Electrode Measurements - A Gilson Oxy5 Oxygraph electrode was used at 22 $^{\circ}\text{C}$. The assays contained 0.1 M potassium phosphate buffer, pH 7.4, 1 μM HO1, 10 μM heme, and either 1 μM CPR, 1 mM NADPH, 5 mM glucose-6-phosphate, 1 unit/mL glucose-6-phosphate dehydrogenase, and 10 μM MGd or 10 mM sodium ascorbate, 2 mM deferoxamine and 400 μM MGd. A dissolved O_2 concentration of 270 μM was used based on calibration of the electrode by consuming a known concentration of

MOL 28407

protocatechuate with protocatechuate 3,4-dioxygenase (Wittaker et al., 1990). Assays to measure the stoichiometry of O₂ consumption by MGd containing 1 mM NADPH and 1 μM CPR, were mixed with repeated additions of 2 μM MGd.

Cytochrome P450 Activity Assays - The activity of CYP4A1 was measured by lauric acid ω-hydroxylation. The incubations were performed as previously described (Hoch et al., 2000), and the reaction mixtures were worked up by solid-phase extraction and analyzed by GC-MS (He et al., 2005). The activities of CYP3A4 and CYP2C9 were measured with Vivid[®] CYP3A4 and CYP2C9 Green Screening Kits (Invitrogen, Carlsbad, CA). These kits employ direct fluorometric assays in a 96-well plate format and were carried out according to the manufacturer's instructions. Wells that did not contain an inhibitor but contained the complete enzyme system plus the fluorescent substrate were used as "100% activity" controls (i.e., uninhibited enzyme activity). The other wells were identical except for the presence of the inhibitor. When indicated in the text, catalase or an NADPH-regenerating system was included in the wells. At the completion of the reactions, the CYP3A4 and CYP2C9 activities were read on a microplate fluorometer (Spectra Max, Sunnyvale, CA) with the excitation set at 485 nm and the emission at 530 nm. The data are expressed as a percentage of the maximum control fluorescence level.

Data Analysis. To determine the IC₅₀ values, the percent inhibition data were fitted to equation (1) by nonlinear regression using the program KaleidaGraph (Synergy Software, Reading, PA):

MOL 28407

$$p = p_{\max} + \frac{p_{\min} - p_{\max}}{1 + (I/IC_{50})^n} \quad (1)$$

where p (percent inhibition) is the relative decrease in enzyme activity due to the inhibitor concentration I , n is the Hill coefficient, $p_{\max} \leq 100$, and $p_{\min} \geq 0$.

Results

Cell Lines Expressing HO1 Constitutively are Sensitive to Induction of Apoptosis by MGd - MGd is a so-called expanded porphyrin (in the texaphyrin family) that contains five nitrogens in the central core instead of the four found in heme (**Fig. 1A**). Its ability to redox cycle (**Fig. 1B**) may induce cell death in sensitive cell lines. Similar to other porphyrins, MGd could potentially induce expression and/or inhibit the activity of HO1. We treated eight hematopoietic tumor-derived cell lines with MGd to determine if it resulted in increased expression of HO1 protein. In Wil-2 and Ramos cell lines, HO1 expression increased 2-fold and 8-fold, respectively, whereas no increase was detected in the other six cell lines (**Fig. 2A**). Interestingly, the two cell lines (HF-1 and Wil-2) that expressed detectable levels of HO1 in the absence of MGd were sensitive to MGd-induced apoptosis whereas the six cell lines that did not constitutively express HO1 did not show similar sensitivity (**Fig. 2B**). It is possible that one or more of the cell lines that show no expression of HO1, either in the absence or presence of MGd, do not have the ability to express HO1. Furthermore, the reason for their lack of sensitivity to MGd is unclear, as CPR was present at similar levels in all the cell lines (data not shown), but presumably involves the action of alternative protective mechanisms.

MOL 28407

MGd Synergizes with SnPPIX to Kill Cells - One possible explanation for the correlation between constitutive expression of HO1 and sensitivity to MGd-induced apoptosis is that MGd might inhibit HO1 activity. Although unlikely based on structural features, another potential explanation is that HO1 degrades MGd into toxic metabolites. To distinguish between these two possibilities, we used SnPPIX to inhibit HO1 activity. If MGd is an inhibitor of HO1, then it might be expected to be more toxic in combination with SnPPIX. However, if HO1 activity is required to metabolize MGd into a toxic metabolite, then the combination of MGd and SnPPIX would be expected to be less toxic than MGd alone. Treatment of HF-1 cells with various combinations of MGd and SnPPIX showed substantially greater killing of cells than treatment with either agent alone as assessed by a marker of apoptosis, annexin V after 24 hours (**Fig. 3A**). The combination index of <1 revealed that treatment with MGd and SnPPIX resulted in synergistic killing (**Fig. 3B**). Combinations of MGd and SnPP that individually induced minimal apoptosis above background were also synergistic in inducing apoptosis after four days (data not shown). These data are consistent with the possibility that MGd inhibits HO1 activity, thereby resulting in cell death

CPR Catalyzed MGd Metabolism - MGd shows significant absorbance at 470 and 740 nm, wavelengths at which HO1 activity can be monitored through the formation of biliverdin (688 nm) or in the BVR coupled assay through the formation of bilirubin (468 nm). In the presence of MGd no detectable bilirubin formation was observed at 468 nm in the HO1 - BVR coupled assay; instead, there was a rapid decay of the 340 nm NADPH peak and the 470 and 740 nm peaks of MGd (data not shown). Removing HO1, heme and BVR from the assays had no effect on the rate of NADPH and MGd disappearance. In

MOL 28407

our assays, reaction of 200 μM NADPH with 10 μM MGd in potassium phosphate buffer (pH 7.4) shows a linear rate of 5 $\mu\text{M min}^{-1}$ that increases dramatically to 300 $\mu\text{M min}^{-1}$ upon addition of 1 μM CPR. This is faster than the initial rate of 0.7 $\mu\text{M min}^{-1}$ previously reported with 250 μM NADPH and 12.5 μM MGd in HEPES/NaCl pH 7.5 buffer (Magda et al., 2001). Electron transfer from NADPH to MGd is accelerated by the presence of CPR to such a degree that all of the available NADPH is consumed in an apparent first order reaction with a half-life of 15 sec while some MGd remains (**Fig. 4A**). To prevent rapid depletion of NADPH, a glucose-6-phosphate dehydrogenase regenerating system was included in the assays. In this situation, the concentration of NADPH remains fixed while all of the MGd is consumed within 1 min (**Fig. 4B**). In the absence of NADPH, there was no CPR-dependent degradation of MGd.

HO1 Inhibition - We utilized quenched HPLC assays to detect biliverdin formation by HO1 in the presence of either MGd or the strong competitive inhibitor SnPPIX (**Fig. 5**) (Drummond and Kappas, 1982). Under the conditions of our assays MGd was a more effective inhibitor, exhibiting 90% inhibition at 10 μM MGd as compared to SnPPIX, which gave 50% inhibition at the same concentration (**Fig. 6**). To determine if CPR was necessary for MGd inhibition of HO1, we used sodium ascorbate as the alternate electron donor in the HO1 coupled oxidation reaction. Here SnPPIX maintains the same level of inhibition while MGd is much less effective, suggesting an alternate mechanism of inhibition from SnPPIX that is amplified in the presence of CPR. Aqueous mannitol (5%), serves as a stabilizer in the solvent in which the MGd was provided, and had no effect on HO1 activity in the absence of MGd, (data not shown). MGd inhibits HO1 activity with $\text{IC}_{50} = 0.2 \mu\text{M}$ (**Fig. 7**). Catalase has been found to prevent MGd cell

MOL 28407

toxicity *in vivo* (Evens et al., 2005a). Addition of catalase plus SOD to the assays to prevent deleterious ROS from degrading heme and interfering with the reaction (Nagababu and Rifkind, 2004) gives rise to only a small recovery of activity with a corresponding increase in the IC_{50} to 0.3 μ M. In contrast, MGd is a much less potent inhibitor (IC_{50} = 4.6 mM) in the reaction supported by ascorbate than in that supported by NADPH/CPR.

CPR activity, as measured by the reduction of cytochrome *c* after the full time course of the HO1 activity assays (15 min), was unaffected by concentrations of MGd at which significant HO1 inhibition was observed. Therefore, inactivation of the electron transfer properties of CPR is ruled out, and HO1 is likely to be inhibited by either a limiting O_2 concentration or by metabolites produced in the CPR-dependent degradation of MGd, which was previously shown to produce free Gd^{3+} and the nonaromatic four-electron reduced macrocycle (Mani et al., 2005).

O₂ Consumption - Using a Clark oxygen electrode we measured the change in the dissolved O_2 concentration under conditions that result in 90% inhibition of HO1. Upon addition of 10 μ M MGd, the concentration of dissolved O_2 decreased rapidly and was completely consumed within 1 min (**Fig. 8**). Over the remaining time course of the assay (15 min) the concentration of dissolved O_2 returned to >50% of the original concentration through diffusion of new O_2 into the reaction chamber. Using ascorbate as the electron donor, 400 μ M MGd results in 40% inhibition of HO1 and was sufficient to decrease the concentration of dissolved O_2 to approximately 40% of the starting concentration.

MOL 28407

In the presence of CPR the stoichiometry of NADPH and O₂ consumption is severely uncoupled from MGd consumption. The amount of NADPH and O₂ consumed was correlated with the amount of MGd to determine the stoichiometry of the reaction. Approximately 38 ± 2 equivalents of NADPH and 42 ± 5 equivalents of O₂ were consumed for every MGd that was lost.

Cytochrome P450 Inhibition - CPR is required for the catalytic activities of other enzymes, most notably for turnover of the cytochrome P450 enzymes. We have therefore investigated whether MGd, through its action on CPR, inhibits the catalytic activities of cytochrome P450 enzymes. Three P450 enzymes, CYP2C9, CYP3A4 and CYP4A1 were selected for these inhibition studies. CYP2C9, and particularly CYP3A4, are responsible for a large proportion of all drug oxidations mediated by the human P450 system (Guengerich, 2005), whereas CYP4A1 is a representative of the class of P450 enzymes responsible for the formation of 20-HETE, an arachidonic acid-derived endogenous vasoconstrictor (Capdevila et al., 2005). The inhibition of CYP4A1-mediated lauric acid ω-hydroxylation by MGd was measured in 100 μM potassium phosphate buffer, alone or in the presence of 10 μg/ml catalase or an NADPH regenerating system. At MGd concentrations of 10 μM and 100 μM, 34% and 98% inhibition was observed, respectively, with similar inhibitory potencies in the three different incubation systems. The IC₅₀ values for CYP4A1, CYP3A4 and CYP2C9 measured in the presence of the NADPH regenerating system were 16, 7 and 3 μM, respectively, all of which are substantially higher values than for the inhibition of HO1 (**Fig. 9**).

Discussion

MOL 28407

MGd, which shows promise as a single agent or in combination with radiotherapy, is now in phase Phase II and III clinical trials (Meyers et al., 2004; Evens et al., 2005b). Some of its anticancer action appears to be due to the formation of ROS that induce necrosis or apoptosis (Evens et al., 2005a). However, many cancer cells are hypoxic and/or contain high concentrations of HO1, a protective enzyme that has been linked to rapid tumor growth as a result of its anti-oxidative and anti-apoptotic properties (Tanaka et al., 2003). HO1 is induced under a number of conditions that cause stress to the cell, including hypoxia, heavy metals, UV radiation, and ROS (Choi and Alam, 1996). The protection conferred by induction of HO1 results not only from a decrease in the deleterious effects of free heme, which include lipid peroxidation and oxygen free radical formation, but also from the properties of bilirubin and CO, the end products of heme metabolism. Bilirubin is a potent free radical scavenger (Stocker et al., 1987), while CO is a signaling molecule that activates pathways that reduce hypertension and increase blood flow to tissues (Kim et al., 2006). There is evidence that HO1 inhibition is cytotoxic and can increase sensitivity of tumor cells to anticancer treatments (Sahoo et al., 2002; Tanaka et al., 2003; Berberat et al., 2005).

Here we show a correlation between HO1 expression and sensitivity to MGd-induced apoptosis, suggesting that MGd might inhibit HO1 activity and thus promote cell death. We provide *in vitro* evidence that MGd inhibits HO1, and demonstrate that this inhibition results from interaction of MGd with the microsomal electron transfer protein CPR. This interaction, which diverts electrons into the reduction of O₂, results in the depletion of NADPH and O₂ and production of ROS (**Fig. 1B**). MGd did not interact directly with HO1, nor was it metabolized by this enzyme. Although HO1 has some tolerance for

MOL 28407

substrate alterations (Ortiz de Montellano and Wilks, 2000), MGd is either too large to fit into the catalytic site or does not satisfy specific requirements for binding within that site. In HO1, the heme is sandwiched between two α -helices and electrostatic interactions between the heme propionates and basic residues at the protein surface confer substrate specificity and reactivity (Schuller et al., 1999). Although zinc protoporphyrin IX pegylated at the positions normally occupied by the propionate groups can inhibit HO1 with a potency similar to that of ZnPPIX (Sahoo et al., 2002), the more extensively altered structure of MGd is apparently incompatible with competitive binding to the protein. Nonetheless, MGd is a strong inhibitor with an IC_{50} in the low μ M range.

In the presence of NADPH, CPR and O_2 , MGd is degraded at an accelerated rate by a process that consumes many equivalents of NADPH and O_2 for each MGd that is metabolized. This reaction depletes the necessary cofactor (NADPH) and one of the substrates (O_2) required for heme oxygenase activity. Previous work has shown that CPR-catalyzed degradation of MGd produces free Gd^{3+} and the four-electron reduced expanded porphyrin (Mani et al., 2005). We have found the stoichiometry of this process to be $\sim 40:40:1$ (NADPH: O_2 :MGd), a ratio that requires a large number of electrons to flow from NADPH into O_2 in an uncoupled manner. MGd thus prefers to react with NADPH indirectly, presumably by accepting one electron at a time from CPR after the NADPH electrons are uncoupled by the flavin prosthetic groups of this enzyme.

CPR is the electron transfer system in the endoplasmic reticulum that supplies the reducing equivalents required by both the heme oxygenases and P450 enzymes (Murataliev et al. 2004). The distribution of CPR in human tissues is thus correlated with

MOL 28407

that of both the HO and P450 enzymes. CPR contains two tightly bound flavin cofactors, an FAD and an FMN (Wang et al., 1997). The FAD accepts two electrons from NADPH while the FMN serves as a one-electron carrier. The ease with which CPR performs one-electron transfers makes it responsible for the toxicity of other reducible compounds, including the antitumor drug doxorubicin and the herbicide paraquat (Bartoszek, 2002; Smith, 1987). In each case, CPR activates them to toxic metabolites via a one-electron reduction. Furthermore, under aerobic conditions, reduced paraquat reacts with O₂ to generate superoxide in a cycle that depletes the intracellular NADPH (Lock and Wilks, 2001).

Other molecules that both inhibit and induce HO1 include NO and SnPPIX. Both molecules induce HO1 through the propagation of free radical cascades. NO inhibits HO1 by binding to the heme iron in place of O₂ (Wang et al., 2003) while SnPPIX competes with heme for binding to the active site (Valaes et al., 1998). The latter has been used to treat neonatal hyperbilirubinemia.

The cytochromes P450 are heme-thiolate containing monooxygenases that are involved in the biosynthesis of various endogenous factors as well as in the metabolism of most drugs and xenobiotics (Guengerich, 2005). The cytochrome P450 enzymes, except for some steroidogenic isoforms, utilize two electrons provided by CPR for the activation of O₂ in their catalytic cycle. CYP3A4 and CYP2C9 are the major P450 enzymes in human liver and intestine (Guengerich, 2005), while CYP4A1 catalyzes the ω -hydroxylation of lauric acid and other fatty acids, including arachidonic acid (Capdevila et al., 2005). Surprisingly, P450 enzymes do not appear to play a role in the metabolism of MGd (Mani et al., 2005). Nevertheless, MGd is a highly effective inhibitor

MOL 28407

of CYP2C9, CYP3A4, and CYP4A1, the three forms examined here. As inhibition of these enzymes also involves diversion of electrons from CPR into uncoupled O₂ reduction, with a consequent depletion of NADPH and oxygen, it is very likely that MGd will also inhibit other CPR-dependent P450 enzymes, at least *in vitro*. Differential inhibition of the three enzymes may reflect a difference in their oxygen affinities or their ability to undergo superoxide-dependent turnover. If MGd were to inhibit P450 enzymes *in vivo*, it might alter the metabolism of other drugs. The physiological relevance of the potential P450 inhibition by MGd is not clear, since in over 500 patients who have received MGd in various clinical trials, no concerns have been raised about potential drug-drug interactions.

MGd disrupts a number of key enzymes important in cellular processes leading to an increase in intracellular free zinc and metallothionein production (Lecane et al., 2005; Magda et al., 2005). It also inhibits thioredoxin reductase, an important antioxidant defense, and ribonucleotide reductase, an enzyme important in DNA synthesis (Hashemy et al., 2006). The ability of MGd to increase oxidative stress to tumor cells, while at the same time inhibiting HO1 and other critical enzymes, may contribute to its effectiveness as an anticancer agent.

MOL 28407

References

- Ali, H., and van Lier, J. E. (1999) Metal complexes as photo- and radiosensitizers. *Chem. Rev.* **99**, 2379-2450.
- Bartoszek, A. (2002) Metabolic activation of adriamycin by NADPH-cytochrome P450 reductase: overview of its biological and biochemical effects. *Acta Biochimica Polonica* **49**, 323-331.
- Berberat, P. O., Dambrauskas, Z., Gulbinas, A., Giese, T., Giese, N., Künzli, B., Autschbach, F., Meuer, S., Büchler, M. W., and Friess, H. (2005) Inhibition of heme oxygenase-1 increases responsiveness of pancreatic cancer cells to anticancer treatment. *Clin. Cancer Res.* **11**, 3790-3798.
- Capdevila, J. H., Holla, V. R., and Falck, J. R. (2005) Cytochrome P450 and the metabolism and bioactivation of arachidonic acid and eicosanoids. In *Cytochrome P450: Structure, Mechanism, and Biochemistry*, 3rd Ed. (Ortiz de Montellano, P. R., Ed.) Plenum, New York, p. 531-551.
- Chen, C., Ramos, J., Sirisawad, M., Miller, R., and Naumovski, L. (2005) Motexafin gadolinium-induces mitochondrially-mediated caspase-dependent apoptosis. *Apoptosis* **10**, 1131-1142.

MOL 28407

Choi, A.M., and Alam, J. (1996) Heme oxygenase-1: function, regulation, and implication of a novel stress-inducible protein in oxidant-induced lung injury. *Am. J. Respir. Cell. Mol. Biol.* **15**, 9-19.

Chou, T.-C., and Talalay, P. (1983) Analysis of combined drug effects: a new look at a very old problem. *Trends Pharmacol. Sci.* **4**, 450-454.

Dierks, E. A., Davis, S. C., and Ortiz de Montellano, P. R. (1998) Glu-320 and Asp-323 are determinants of the CYP4A1 hydroxylation regioselectivity and resistance to inactivation by 1-aminobenzotriazole. *Biochemistry* **37**, 1839-1847.

Drummond, G. S., and Kappas, A. (1982) Chemoprevention of neonatal jaundice: potency of tin-protoporphyrin in an animal model. *Science* **217**, 1250-1252.

Evens, A. M., Lecane, P., Magda, D., Prachand, S., Singhal, S., Nelson, J., Miller, R. A., Gartenhaus, R. B., and Gordon, L. I. (2005a) Motexafin gadolinium generates reactive oxygen species and induces apoptosis in sensitive and highly resistant multiple myeloma cells. *Blood* **105**, 1265-1273.

Evens, A. M., Balasubramanian, L., and Gordon, L. I., (2005b) Motexafin gadolinium induces oxidative stress and apoptosis in hematologic malignancies. *Curr. Treat. Options. Oncol.* **6**, 289-296.

Guengerich, F. P. (2005) Human cytochrome P450 enzymes. In *Cytochrome P450: Structure, Mechanism, and Biochemistry*, 3rd Ed. (Ortiz de Montellano, P. R., Ed.) Plenum, New York, p. 377-530.

MOL 28407

- Hashemy, S. I., Ungerstedt, J. S., Avval, F. Z., and Holmgren, A. (2006) Motexafin gadolinium: A tumor selective drug targeting thioredoxin reductase and ribonucleotide reductase. *J. Biol. Chem.* **281**, 10691-10697.
- He, X., Cryle, M. J., De Voss, J. J., and Ortiz de Montellano, P. R. (2005) Calibration of the channel that determines the ω -hydroxylation regiopecificity of cytochrome P4504A1. Catalytic oxidation of 12-halododecanoic acids. *J. Biol. Chem.* **280**, 22697-22705.
- Hoch, U., Zhang, Z., Kroetz, D. L., and Ortiz de Montellano, P. R. (2000) Structural determination of the substrate specificities and regioselectivities of the rat and human fatty acid ω -hydroxylases. *Arch. Biochem. Biophys.* **373**, 63-71.
- Kim, H. P., Ryter, S. W., and Choi, A. M. (2006) CO as a cellular signaling molecule. *Annu. Rev. Pharmacol. Toxicol.* **46**, 411-449.
- Lecane, P. S., Karaman, M. W., Sirisawad, M., Naumovski, L., Miller, R. A., Hacia, J. G., Magda, D. (2005) Motexafin gadolinium and zinc induce oxidative stress responses and apoptosis in B-cell lymphoma lines. *Cancer Res.* **65**, 11676-11688.
- Lock, E. A., and Wilks, M. F. (2001) Paraquat. In *Handbook of pesticide toxicology*. (Krieger, R. I., Ed.) Academic Press, San Diego, p. 1559-1603.
- Madga, D., Lepp, C., Gerasimchuk, N., Lee, I., Sessler, J. L., Lin, A., Biaglow, J. E., and Miller, R. A. (2001) Redox cycling by motexafin gadolinium enhances cellular

MOL 28407

- response to ionizing radiation by forming reactive oxygen species. *Int. J. Radiat. Oncol. Biol. Phys.* **51**, 1025-1036.
- Magda, D., Gerasimchuk, N., Lecane, P., Miller, R. A., Biaglow, J. E., and Sessler, J. L. (2002) Motexafin gadolinium reacts with ascorbate to produce reactive oxygen species. *Chem. Commun.* 2730-2731.
- Magda, D., Lecane, P., Miller, R. A., Lepp, C., Miles, D., Mesfin, M., Biaglow, J. E., Ho, V. V., Chawannakul, D., Nagpal, S., Karaman, M. W., and Hacia, J. G. (2005) Motexafin gadolinium disrupts zinc metabolism in human cancer cell lines. *Cancer Res.* **65**, 3837-3845.
- Mani, C., Upadhyay, S., Lacy, S., Boswell, G. W., and Miles, D. R. (2005) Reductase-mediated metabolism of motexafin gadolinium (Xcytrin) in rat and human liver subcellular fractions and purified enzyme preparations. *J. Pharm. Sci.* **94**, 559-570.
- Margoliash, E., and Walasek, O. F. (1967) Cytochrome *c* from vertebrate and invertebrate sources. *Methods Enzymol.* **10**, 339-348.
- Meyers, C. A., Smith, J. A., Bezjak A., Mehta, M. P., Liebmann, J., Illidge, T., Kunkler, I., Caudrelier, J. M., Eisenberg, P. D., Meerwaldt, J., Siemers, R., Carrie, C., Gaspar, L. E., Curran, W., Phan, S. C., Miller, R. A., and Renschler, M. F. (2004) Neurocognitive function and progression in patients with brain metastases treated

MOL 28407

- with whole-brain radiation and motexafin gadolinium: results of a randomized phase III trial. *J. Clin. Oncol.* **22**, 157-165.
- Murataliev, M. B., Feyereisen, R., and Walker, A. (2004) Electron transfer by diflavin reductases. *Biochim. Biophys. Acta – Proteins & Proteomics* **1698**, 1-26.
- Nagababu, E., and Rifkind, J. M. (2004) Heme degradation by reactive oxygen species. *Antioxid Redox Signal* **6**, 967-978.
- Ortiz de Montellano, P. R., (1998) Heme oxygenase mechanism: evidence for an electrophilic, ferric peroxide species. *Acc. Chem. Res.* **31**, 543-549.
- Ortiz de Montellano, P. R., and Wilks, A. (2000) Heme oxygenase structure and mechanism. In “Iron Porphyrins”, *Advances in Inorganic Chemistry* (Sykes, G., and Mauk, A. G., Eds.) **51**, 359-407.
- Sahoo, S. K., Sawa, T., Fang, J., Tanaka, S., Miyamoto, Y., Akaike, T., and Maeda, H. (2002) Pegylated zinc protoporphyrin: a water-soluble heme oxygenase inhibitor with tumor-targeting capacity. *Bioconjugate Chem.* **13**, 1031-1038.
- Schuller, D. J., Wilks, A., Ortiz de Montellano, P. R., and Poulos, T. L. (1999) Crystal structure of human heme oxygenase-1. *Nat. Struct. Biol.* **6**, 860-867.
- Smith, L. L. (1987) Mechanism of paraquat toxicity in lung and its relevance to treatment. *Hum. Toxicol.* **6**, 31-36.

MOL 28407

Stocker, R., Yamamoto, Y., McDonagh, A. F., Glazer, A. N., and Ames, B. N. (1987)

Bilirubin is an antioxidant of possible physiological importance. *Science* **235**, 1043-1046.

Tanaka, S., Akaike, T., Fang, J., Beppu, T., Ogawa, M., Tamura, F., Miyamoto, Y., and

Maeda, H. (2003) Antiapoptotic affect of haem oxygenase-1 induced by nitric oxide in experimental solid tumor. *Br. J. Cancer* **88**, 902-909.

Tomaro, M. L., Frydman, R. B., Frydman, B., Pandey, R. K., and Smith, K. M. (1984)

The oxidation of hemins by microsomal heme oxygenase. Structural requirements for the retention of substrate activity. *Biochim. Biophys. Acta*, **791**, 342-349.

Valaes, T., Drummond, G., and Kappas, A. (1998) Control of hyperbilirubinemia in

glucose-6-phosphate dehydrogenase-deficient newborns using an inhibitor of bilirubin production, Sn-mesoporphyrin. *Pediatrics* **101**, E1-E7.

Vlahakis, J Z., Kinobe, R. T., Bowers, R. J., Brien, J. F., Nakatsu, K., and Szarek, W. A.

(2005) Synthesis and evaluation of azalanstat analogues as heme oxygenase inhibitors. *Bioorg. Med. Chem. Lett.* **15**, 1457-1461.

Wang, M., Roberts, D. L., Paschke, R., Shea, T. M., Masters, B. S. S., and Kim, J.-J. P.

(1997) Three-dimensional structure of NADPH-cytochrome P450 reductase: prototype for FMN- and FAD-containing enzymes. *Proc. Natl. Acad. Sci. U.S.A.* **94**, 8411-8416.

MOL 28407

Wang, J., Lu, S., Moëne-Loccoz, P., and Ortiz de Montellano, P. R. (2003) Interaction of nitric oxide with human heme oxygenase-1. *J. Biol. Chem.* **278**, 2341-2347.

Wilks, A., Black, S. M., Miller, W. L., and Ortiz de Montellano, P. R. (1995) Expression and characterization of truncated human heme oxygenase (hHO-1) and a fusion protein of hHO-1 with human cytochrome P450 reductase. *Biochemistry* **34**, 4421-4427.

Wittaker, J. W., Orville, A. M., and Lipscomb, J. D. (1990) Protocatechuate 3,4-dioxygenase from *Brevibacterium fuscum*. *Methods Enzymol.* **188**, 82-88.

Young, S. W., Qing, F., Harriman, A., Sessler, J. L., Dow, W. C., Mody, T. D., Hemmi, G. W., Hao, Y., and Miller, R. A. (1996) Gadolinium(III) texaphyrin: a tumor selective radiation sensitizer that is detectable by MRI. *Proc. Natl. Acad. Sci. U. S. A.* **93**, 6610-6615.

MOL 28407

FOOTNOTES

Title footnote: This work was supported by National Institute of Health grants Dk30297 and GM25515.

*To whom correspondence should be addressed: ortiz@cgl.ucsf.edu

MOL 28407

FIGURE LEGENDS

Figure 1. **A.** Structure of MGd. **B.** Reaction catalyzed by MGd with O₂ and reducing equivalents from NADPH.

Figure 2. **A.** Western blot for HO1 in MGd treated hematopoietic tumor-derived cell lines. Cells were grown in the presence (+) or absence (-) of 50 μM MGd for 24 h. Protein extracts were separated by SDS-PAGE and western blotting was performed with antibodies to HO1. Hsc70 was used as an internal loading standard. **B.** Cells were grown in the presence (+) or absence (-) of 50 μM MGd for 4 days. Numbers of apoptotic cells were quantitated by FITC-annexin V binding using flow cytometry.

Figure 3. **A.** MGd and SnPPIX synergize to kill HF-1 cells. HF-1 cells were treated with various concentrations of MGd, SnPPIX or combinations of the drugs for 24 h. Apoptosis was quantitated by assay for annexin V binding. **B.** Combination index (CI) plot showing CI < 1, consistent with synergistic interaction between MGd and SnPPIX. The center curve is the calculated CI with the boundary lines representing +/- 1.96 standard deviations for 95% certainty.

Figure 4. Spectroscopic changes in the presence of **(A)** 200 μM NADPH, 1 μM CPR, and 10 μM MGd showing an initial rate of NADPH consumption of 300 μM/min and MGd consumption of 11 μM/min; **(B)** Addition of the NADPH regeneration system maintains NADPH levels while MGd consumption shows the same initial rate of disappearance. The time scale of the reactions was 60 s, with spectra shown at 10 s intervals.

MOL 28407

Figure 5. HPLC chromatogram showing MGd and SnPPIX inhibition of HO1. Assays contained 1 μ M HO1, 10 μ M heme, 1 μ M CPR, 1 mM NADPH, 5 mM glucose-6-phosphate, 1 unit/mL of glucose-6-phosphate dehydrogenase and the indicated amount of inhibitor. Unreacted heme elutes as the FePPIX dimethyl ester (FePPIXDME) at ~26 min and biliverdin dimethyl ester (BVDME) at ~28 min.

Figure 6. Relative inhibition of HO1 in the presence of SnPPIX or MGd with either NADPH/CPR or ascorbate as the electron donor.

Figure 7. MGd inhibition of HO1 activity with NADPH/CPR in the presence (\blacktriangle) and absence (\bullet) of 10 μ g/ml catalase and 17 units/ mL SOD gives IC_{50} values of 0.3 μ M and 0.2 μ M, respectively. Assays contained 1 μ M HO1, 10 μ M heme, and either 1 μ M CPR, 1 mM NADPH, and an NADPH regenerating system or 10 mM sodium ascorbate and 2 mM deferoxamine. Using ascorbate as the reductant (\blacksquare) the IC_{50} increases to 4.6 mM.

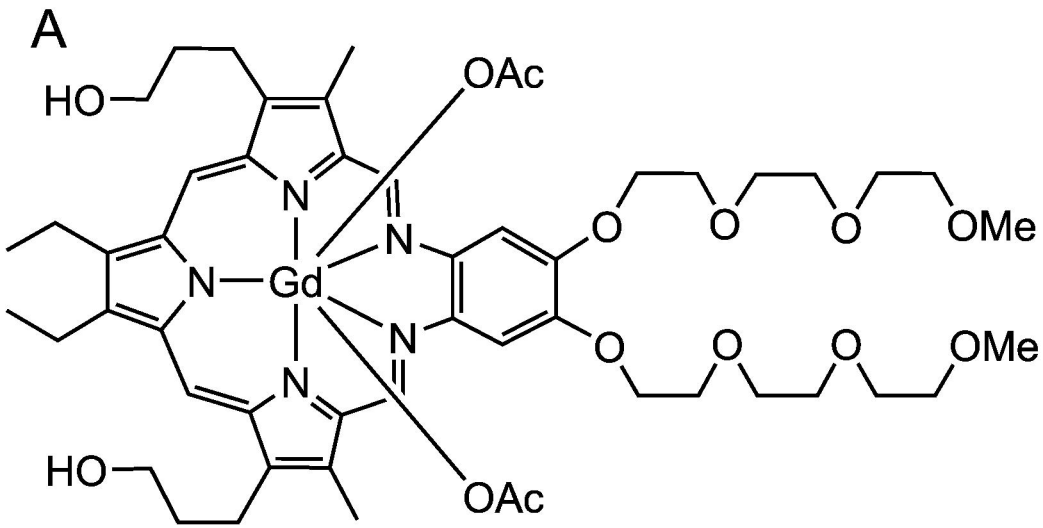
Figure 8. Oxygen electrode trace showing the consumption of O_2 upon addition of 10 μ M MGd to a reaction containing 1 μ M HO1, 10 μ M heme, 1 μ M CPR, 1 mM NADPH, 5 mM glucose-6-phosphate, and 1 unit/mL of glucose-6-phosphate dehydrogenase (solid line), or 400 μ M MGd to a reaction containing 1 μ M HO1, 10 μ M heme, 10 mM ascorbate, and 2 mM DFA (dotted line). Omission of HO1 and heme from the assays resulted in similar O_2 consumption profiles (not shown).

Figure 9. MGd inhibition of CYP4A1(\bullet), CYP3A4(\blacktriangle) and CYP2C9(\blacksquare) activity in a system consisting of NADPH/CPR plus the NADPH regenerating system. The IC_{50} 's of MGd in these three systems are 16, 7 and 3 μ M, respectively. CYP4A1 assays contained

MOL 28407

100 μ M lauric acid, 0.1 μ M CYP450, 1 mM NADPH, 1 μ M CPR and the NADPH regenerating system. CYP3A4 and CYP2C9 assays contained 5 nM and 10 nM CYP450 BACULOSOMES[®] Reagent, respectively, 2 μ M Vivid[®] CYP450 Substrate, 100 μ M NADP⁺ and regeneration system.

Figure 1



B

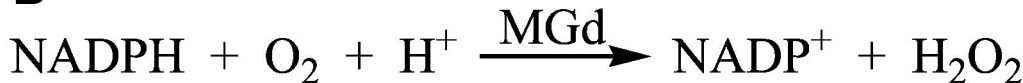


Figure 2

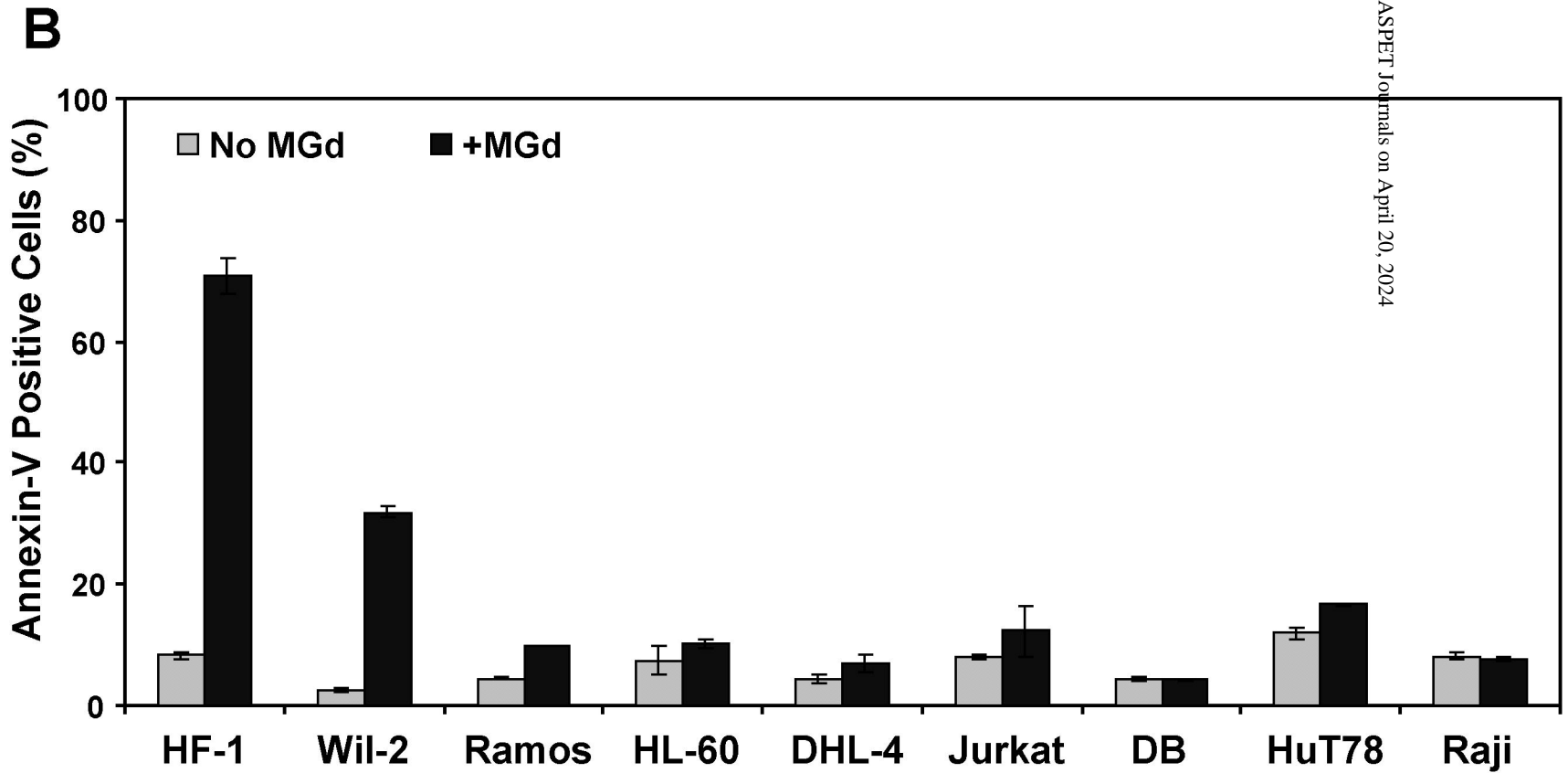
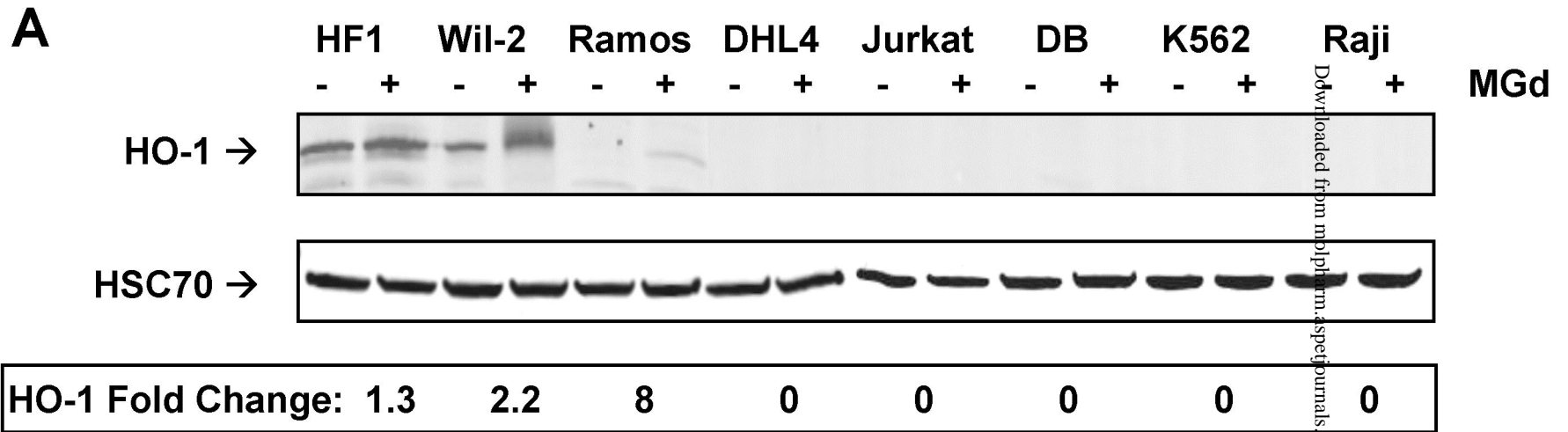
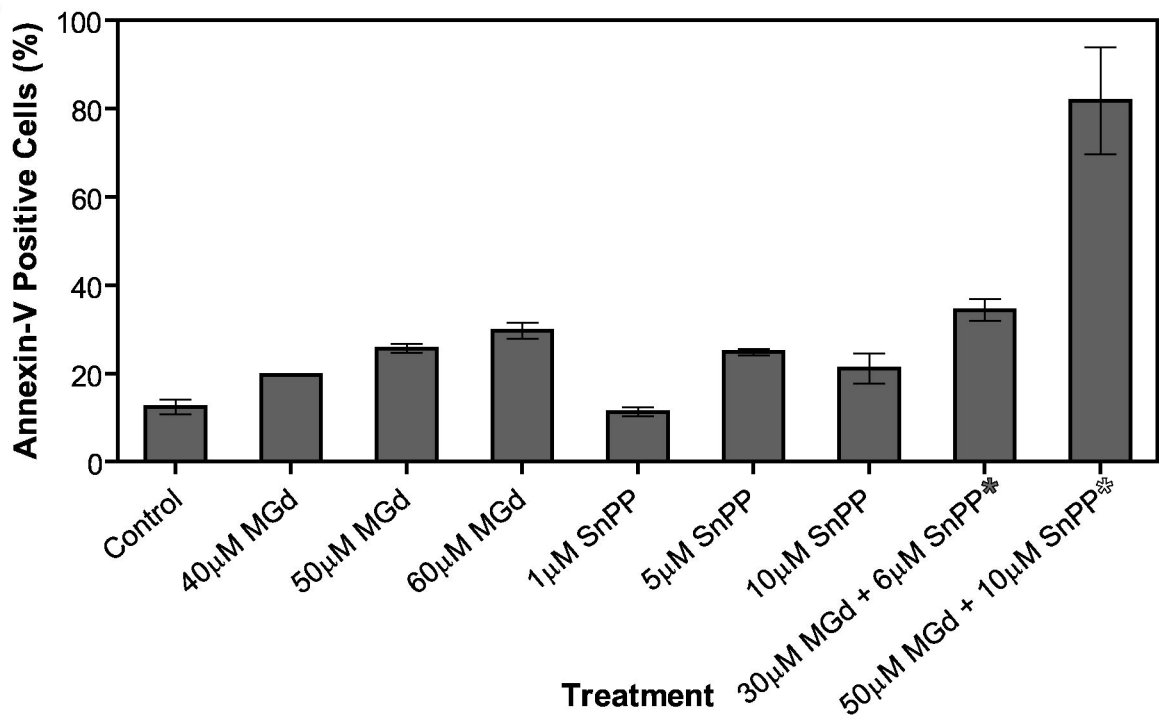


Figure 3

A



B

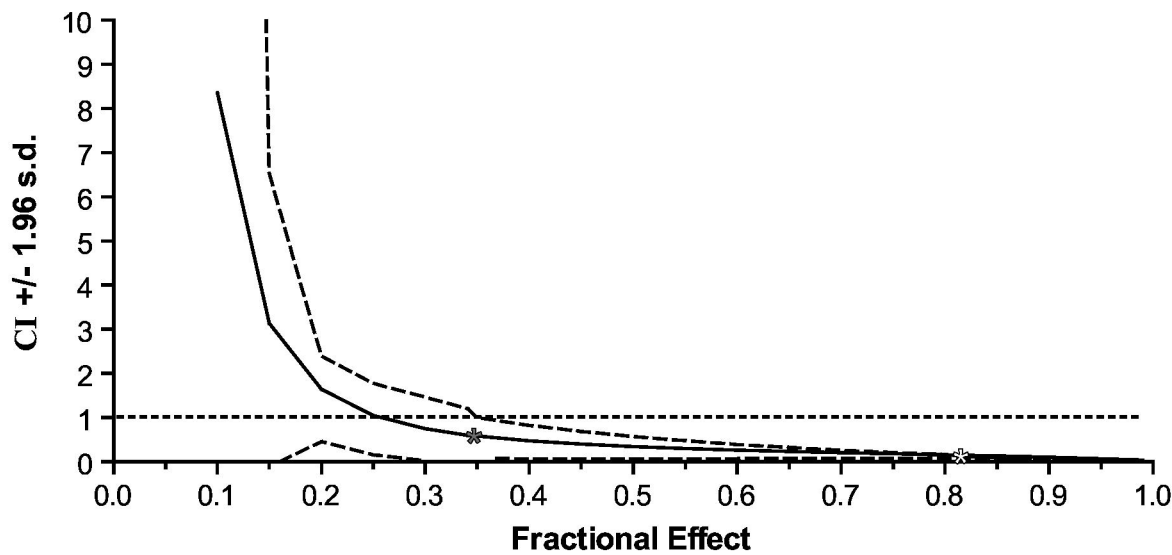


Figure 4

Molecular Pharmacology Fast Forward. Published on October 3, 2006 as DOI: 10.1124/mol.106
This article has not been copyedited and formatted. The final version may differ from this version.

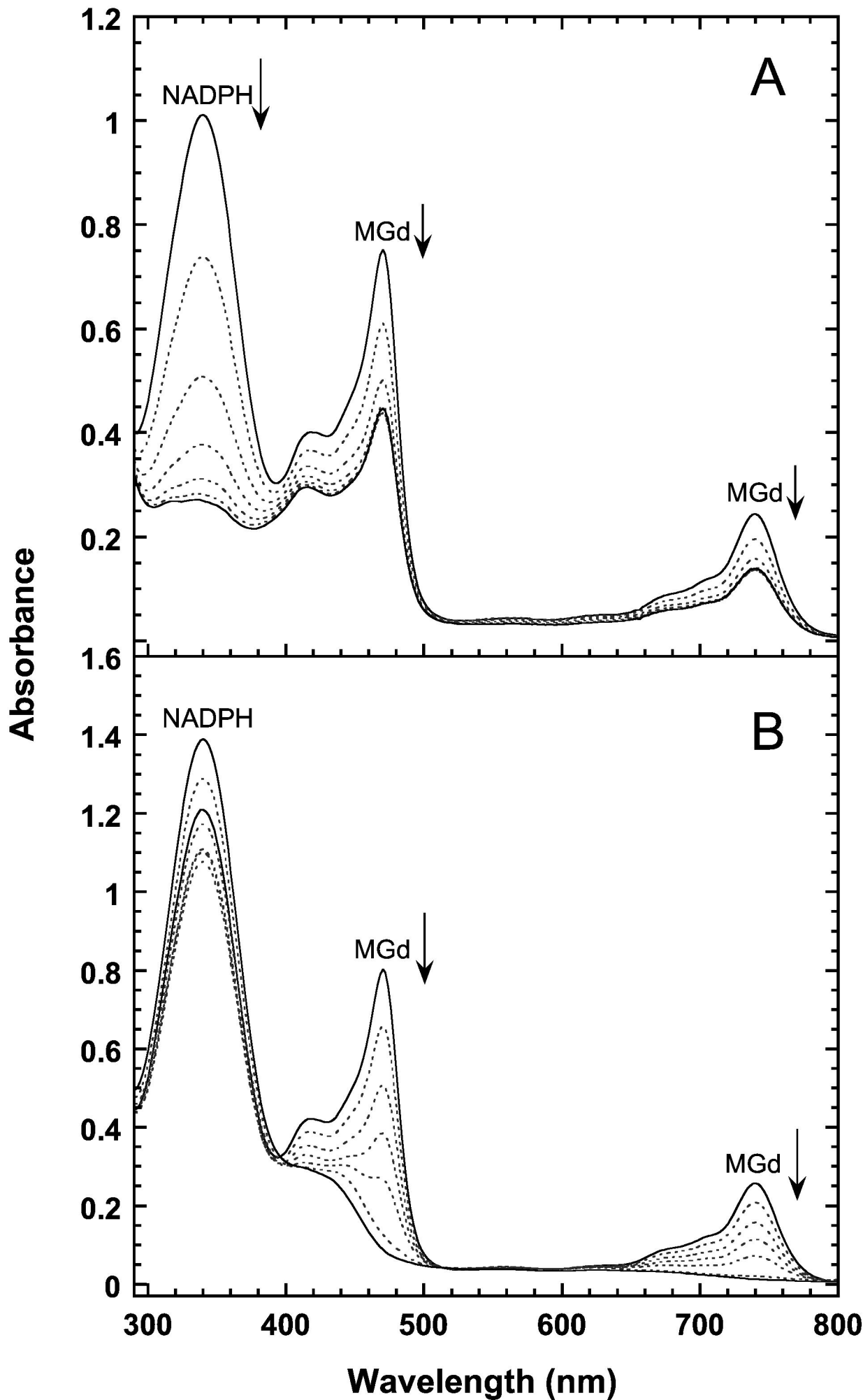


Figure 5

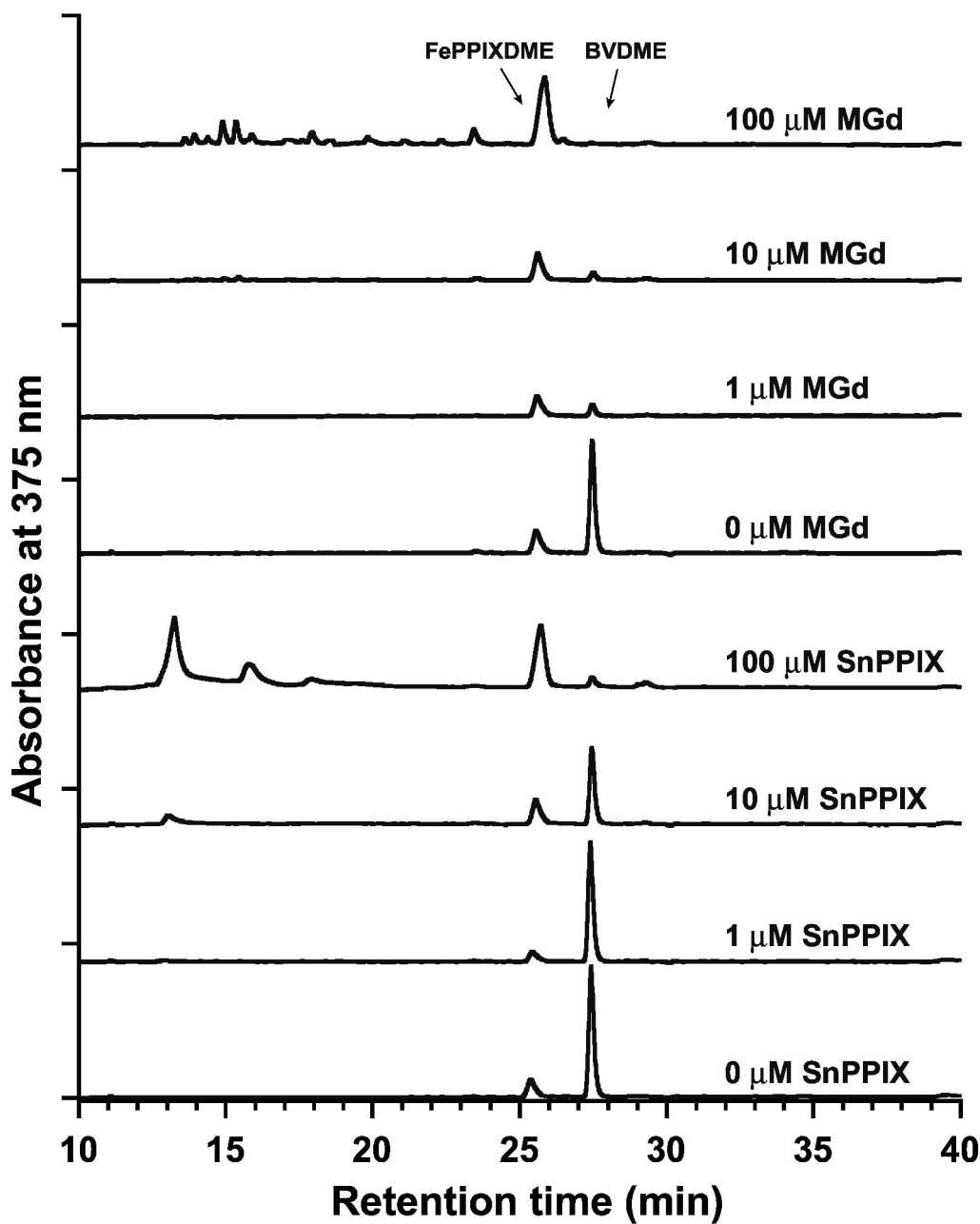


Figure 6

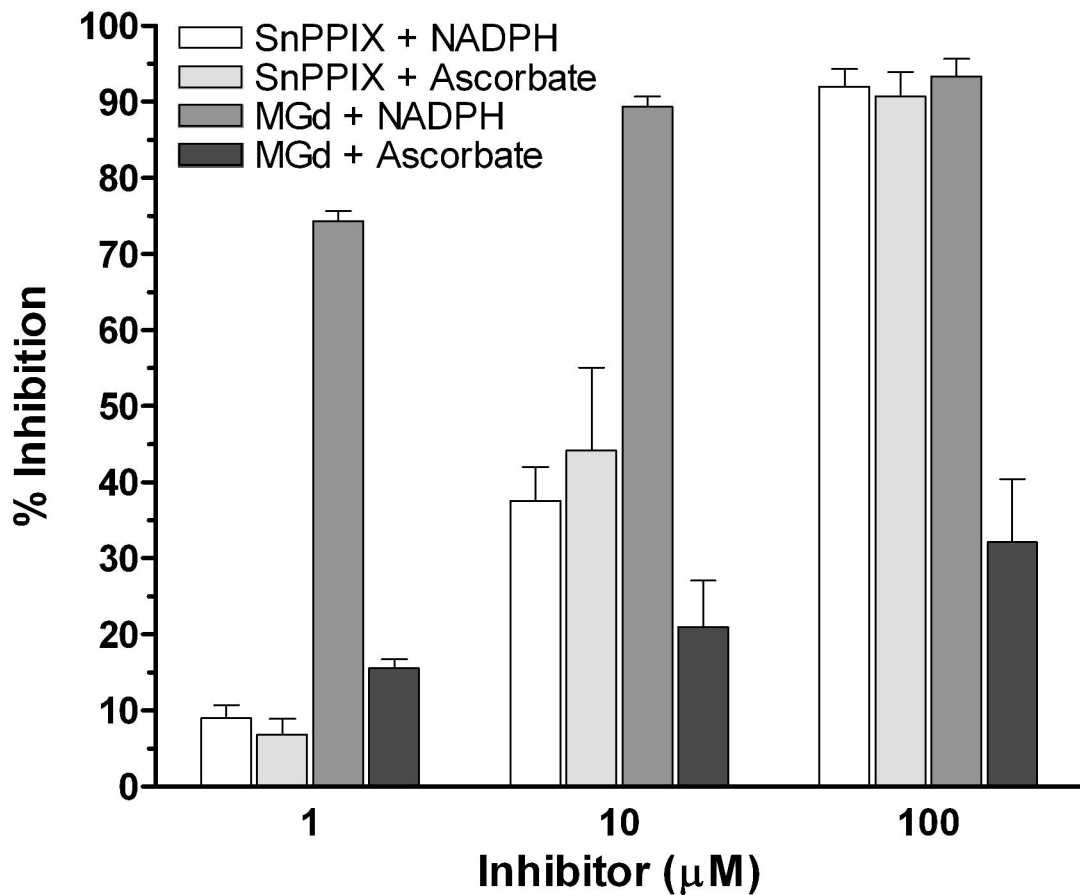


Figure 7

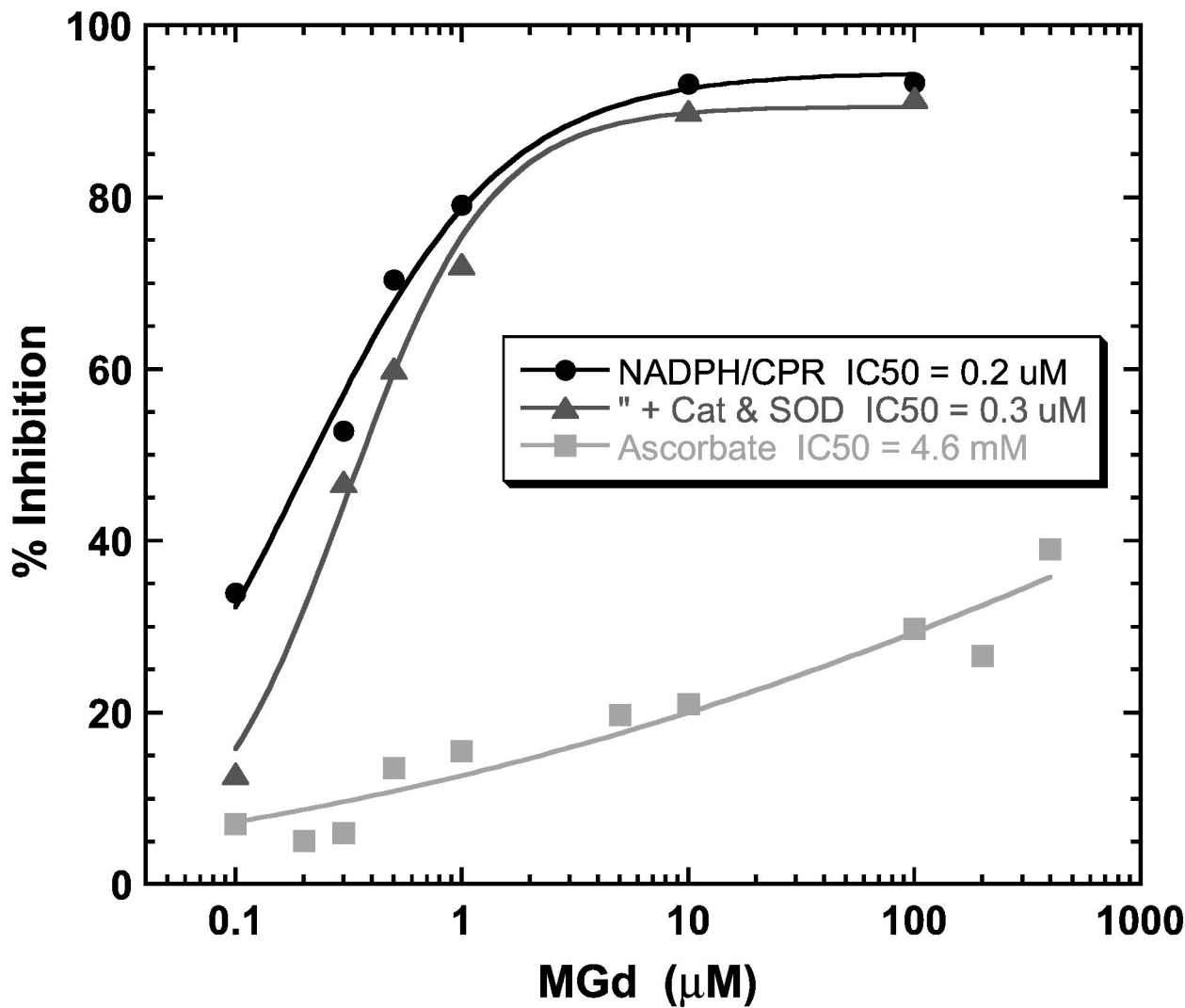


Figure 8

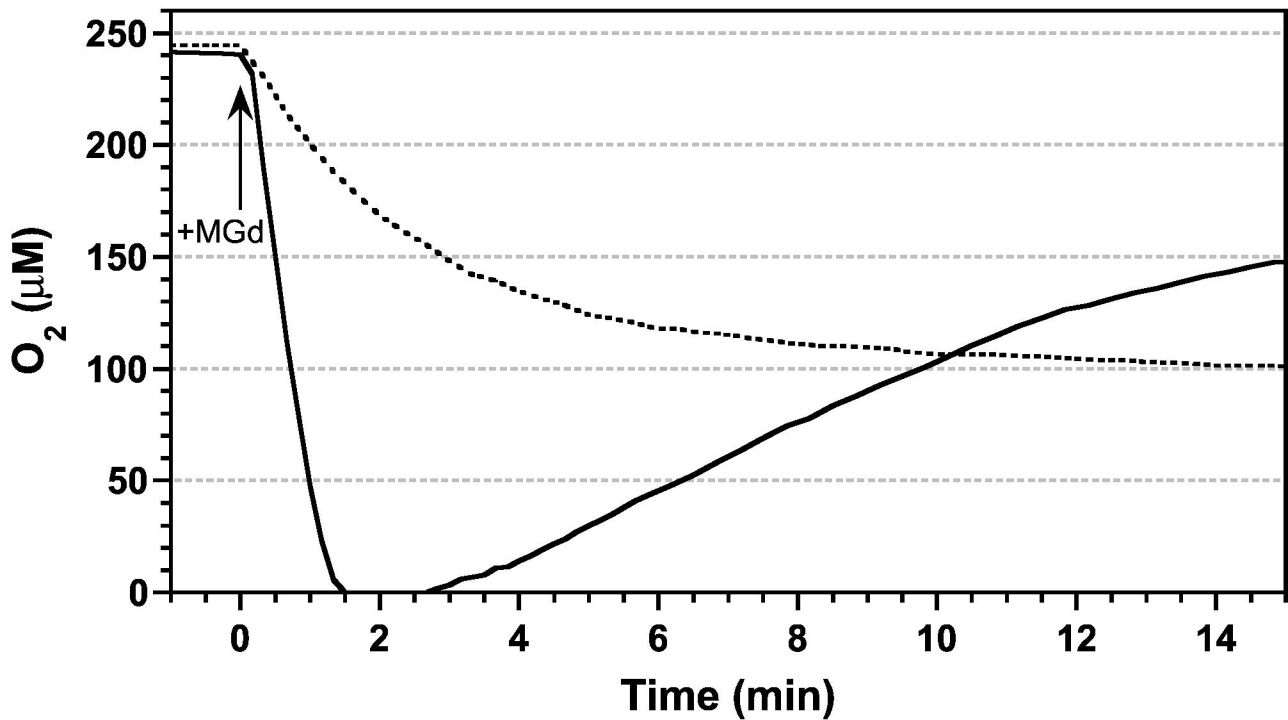


Figure 9

